ADVANCED DINSAR TECHNIQUES FOR MONITORING TERRAIN DISPLACEMENTS

Oscar Mora; Roman Arbiol and Vicenç Palà

Institut Cartogràfic de Catalunya (ICC). Parc de Montjuïc s/n, 08038 Barcelona. omora@icc.es

KEY WORDS: Radar, SAR, InSAR, DInSAR, subsidence, earthquake, interferometry.

INTRODUCTION

This paper presents an advanced DInSAR technique developed by the Cartographic Institute of Catalonia (ICC) for the generation of precise terrain deformation maps using data acquired by satellite platforms. These radar systems, known as Synthetic Aperture Radar (SAR), allow obtaining terrain reflectivity images, which are processed by means of DInSAR algorithms for monitoring ground stability. The great advantage of these techniques relies on the possibility of monitoring large areas with no need of field measurements and at low cost. This work presents several results obtained with the DISICC (Differential Interferometry SAR ICC) software developed at ICC.

DIFFERENTIAL INTERFEROMETRY (DInSAR)

DInSAR techniques consist of the combination of two SAR images of the same area acquired from slightly different positions, see Fig. 1.

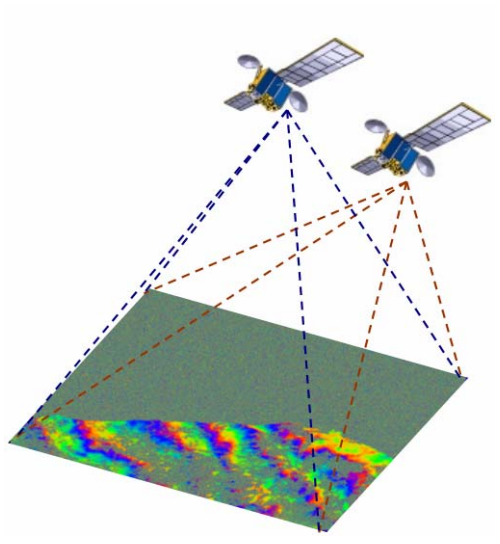

Figure 1 – DInSAR acquisition scheme.

The result of this combination is a new image known as interferogram, whose phase component is formed by the following terms:

$$\Delta\Phi_{Int} = \Phi_{Topo} + \Phi_{Mov} + \Phi_{Atm} + \Phi_{Noise} \quad (1)$$

where Φ_{Topo} is the term related with topography, Φ_{Mov} is the phase component of terrain deformation, Φ_{Atm} is the noise component caused by different atmospheric conditions for both SAR acquisitions and Φ_{Noise} is the thermal noise.

Topography, atmospheric effects and thermal noise must be canceled or minimized to obtain precise measurements of terrain movement. When working with classical DInSAR interferograms (combination of two SAR images) the main problem is the presence of atmospheric artifacts, since there is no way to cancel them without a priori information. On the other hand, the term related with topography can be canceled using and external Digital Elevation Model (DEM) and the orbital parameters of the SAR acquisitions, considering no height errors on the DEM, see (2).

$$\Delta\Phi_{dif} = \Phi_{ErrorTopo} + \Phi_{Mov} + \Phi_{Atm} + \Phi_{Noise} \quad (2)$$

As conclusion, atmospheric artifacts and DEM errors will affect the measurement precision on the deformation velocity. For this reason, classical DInSAR can be only applied with fast subsidences, such as earthquakes, where the temporal interval between SAR acquisitions can be very low and the deformation signal is much stronger than atmospheric artifacts and DEM errors.

ADVANCED DInSAR

The DISICC software has been created to overcome these inherent limitations of classical DInSAR using a stack of interferometric pairs with SAR images acquired at different dates. The redundancy obtained with these data allows the minimization of the atmospheric artifacts and topographic errors. The main characteristics of the software developed at ICC are the following:

- The first step of the process consists of a selection of those pixels that present high levels of coherence (phase quality) during the temporal interval of SAR acquisitions. Those areas that preserve their electromagnetic behavior will be selected, such as urban, arid or rock zones. On the other hand, the pixels related with vegetated areas will be usually rejected due to their low coherence level. Note that when combining images with large temporal separation high coherence is only preserved on electromagnetically stable zones.
- A triangulation process is carried out after pixel selection for relating neighboring points. The

information is not present in the absolute phase, but in the phase increments between adjacent points. An advantage of this processing is the minimization of atmospheric artifacts, since atmosphere is a low frequency signal in space.

- A phase model depending on the number of interferograms is adjusted to data using the following minimization function:

$$\Gamma = \frac{1}{N} \cdot \left| \sum_{i=0}^{N} \exp\left[j \cdot \left(\Phi_{dif} - \Phi_{\text{model}} \right) \right] \right| \qquad (3)$$

- Φ_{model} is the differential interferometric phase model that depends on the temporal and spatial separation of SAR acquisitions that form each interferogram and *N* is the number of interferograms.
- After minimizing the function in (3) we obtain the increment values of topographic error and deformation velocity that best fit the network created by the triangulation commented above. Then, an integration process is needed to get their absolute values for each point.
- The next step consists of the subtraction of the estimated model from each interferogram. The result is a phase residue formed by the non-linear components of the terrain displacement that are not taken into account in the simplified model used in (3).
- Finally, these residues must be re-ordered in time and added to the model for obtaining the complete description of the temporal evolution of the deformation.

Using the algorithm described above precise estimations of terrain displacements can be performed due to the amount of information present in *N* interferograms. The greater the number of images, the better the result precision. Our experience processing these kind of data says that a standard deviation lower than 3 mm/year or 5mm in absolute deformation can be obtained with stack of images larger than 20.

RESULTS

In this section several results are presented for both classical and advanced DInSAR. The first example corresponds to the Al-hoceima (Morocco) earthquake that took place on 24 February 2004 with a magnitude Mw 6.5. For this case two ENVISAT images has been processed, acquired on 23 July 2003 and 28 April 2004. Figure 2 shows the deformation fringes related with the rupture caused by the earthquake. It is very clear the coast area affected by the stronger magnitude of the displacement. Note that each color cycle corresponds to 2.8 cm of terrain movement.

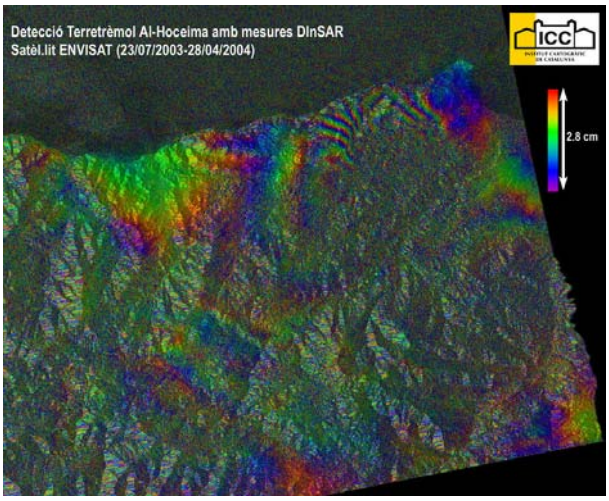

Figure 2 – Interferometric phase pattern of the. Al-hoceima earthquake (24 February 2004, Mw 6.5).

The second example corresponds to an area of Catalonia affected by mining exploitations. Figure 3 clearly shows three subsidence areas in the interferogram generated with images acquired at 3 February 2005 and 19 May 2005. It is important to remark that in this case several deformation phase fringes, 2.8 cm each color cycle, appear in only three months of temporal gap. This demonstrates the strong subsidence caused by this kind of exploitations.

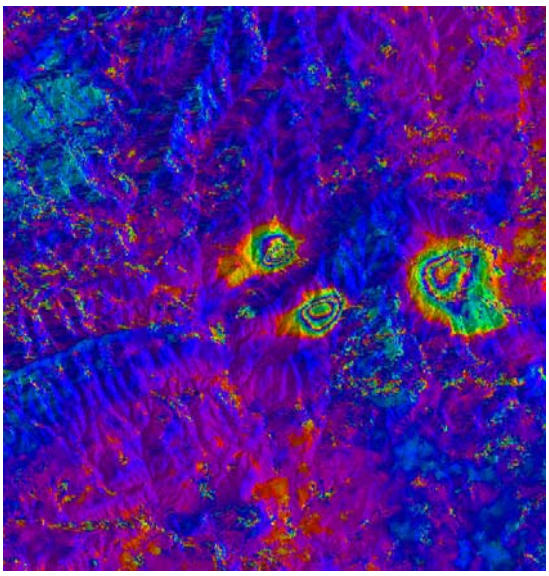

Figure 3 – Interferometric phase pattern of three deformation areas located in Catalonia due to mining activities.

The last example presented in this paper has been generated using advanced DInSAR techniques implemented in DISICC software. A stack of SAR images acquired at different dates from slightly different positions has been used.

The area under study is Sallent, a town located in the center of Catalonia. An old mine is found in the south part of this area generating strong subsidence problems in a neighborhood. Figure 4 shows the subsidence map estimated with DISICC where the shape and magnitude of this deformation are clearly depicted. Note that those zones with no representation of color points correspond to low coherence areas that are not selected in the first step of the algorithm presented in the previous section.

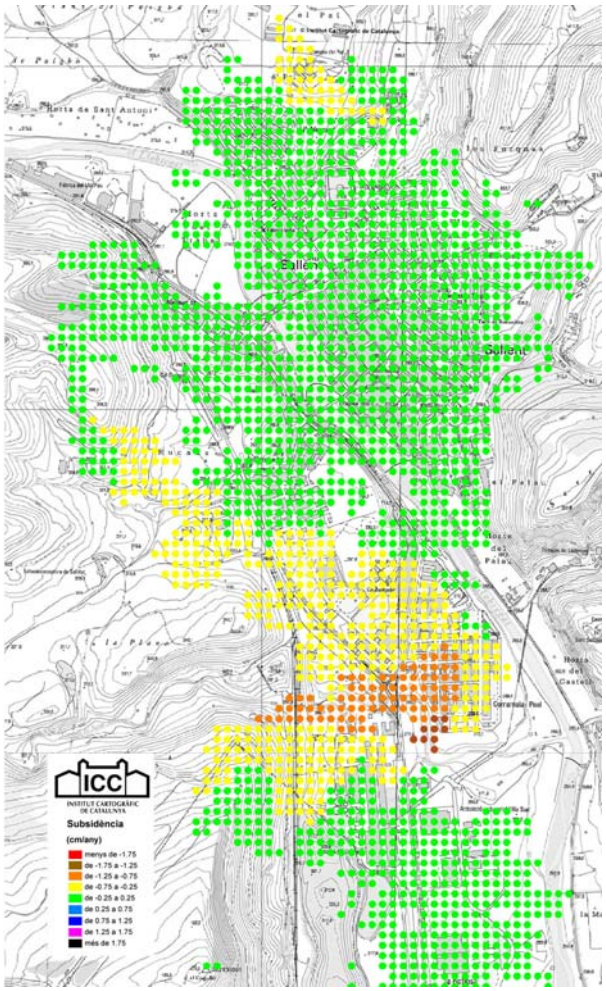

Figure 4 – Deformation velocity estimated using DISICC software (Advanced Differential Interferometry) in Sallent. Green points are stable and brown ones have maximum displacement.

Finally, Figure 5 presents a comparison between leveling measurements and DISICC results of the temporal behavior of deformation in the area of maximum velocity. This result shows the extraordinary fitting of absolute deformation measurements using these two different techniques. The advantage of advanced DInSAR relies on the capability of monitoring large areas with reduced costs compared with expensive field campaigns.

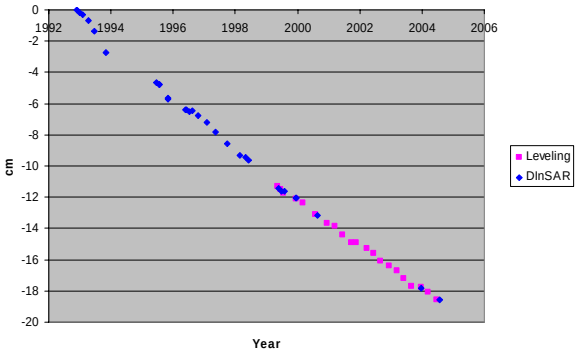

Figure 5 – Combination of advanced DInSAR and leveling measurements for one point in the maximum deformation area of Sallent.

CONCLUSIONS

This paper presents DISICC software for advanced DInSAR processing focused on precise estimation of terrain deformations. This software takes advantage of stack image processing to minimize decorrelation factors. Several results are presented demonstrating the capabilities of this technique and its future use on risk management.

BIBLIOGRAPHY

MORA, O., MALLORQUÍ, J., BROQUETAS, A, 2003. Linear and Nonlinear Terrain Deformation Maps From a Reduced Set of Interferometric SAR Images. IEEE Transactions on Geoscience and Remote Sensing, Vol. 41, No. 10.

LANARI, R., MORA, O., MANUNTA, M., MALLORQUÍ, J., BERARDINO, P., SANSOSTI, E., 2004. A Small Baseline DIFSAR Approach for Investigating Deformations on Full Resolution SAR Interferograms. IEEE Transactions on Geoscience and Remote Sensing, Vol. 42, No. 7.

MORA, O., PALÀ, V., ARBIOL, R., ADELL, A., TORRE, M., 2005. Medidas de deformación del terreno a vista de satélite. XI Congreso Nacional de Teledetección, Puerto de la Cruz, Tenerife.

MASSONET, D., 1993. The displacement field of the Landers earthquake mapped by radar interferometry. Nature, Vol. 364, pp. 138-142.